Inorganic Chemistry

Article

pubs.acs.org/IC

Al-Induced Crystallization of Amorphous Ge and Formation of Fractal Ge Micro-/Nanoclusters

Quanbao Li,[†] Chen Chen,[†] Zhiwen Chen,[†,§,*] Zheng Jiao,[†,‡,*] Minghong Wu,[†,‡,*] Chan-Hung Shek,[§] C. M. Lawrence Wu,[§] and Joseph K. L. Lai[§]

[†]Shanghai Applied Radiation Institute and [‡]Institute of Nanochemistry and Nanobiology, School of Environmental and Chemical Engineering, Shanghai University, Shanghai 200444, People's Republic of China

[§]Department of Physics and Materials Science, City University of Hong Kong, Tat Chee Avenue, Kowloon Tong, Hong Kong

ABSTRACT: Results on Al-induced crystallization of amorphous Ge (a-Ge) deposited by vacuum thermal evaporation techniques under thermal annealing in N_2 atmosphere are presented in detail. The a-Ge crystallization and fractal Ge pattern formation on the free surface of annealed Al/Ge bilayer films deposited on single-crystal Si (100) substrates were investigated by using scanning electron microscopy (SEM), X-ray diffraction (XRD), atomic force microscopy (AFM), energy dispersive X-ray spectrometry (EDS), and Raman spectra. It is found that the temperature field effects play an extremely crucial role in a-Ge crystallization and fractal Ge formation process. The open branched structure of fractal Ge clusters in Al/Ge bilayer films was effectively prepared by Al-induced crystallization when they were annealed at 400 °C for 60 min. These films with fractal Ge clusters exhibit charming noninteger dimensional nanostructures, which differ from those of conventional integer dimensional materials such as one-dimensional nanowires/nanorods, nanotubes, nanobelts/nanoribbons, two-dimensional heterojunctions, thin films, and zero-dimensional nanoparticles. The SEM image shows that a big Al grain was found located near the center of a fractal Ge cluster after the films were annealed at 400 and 500 °C for 60 min. This suggests that the grain boundaries of polycrystalline Al films are the initial nucleation sites of a-Ge. It also validates the preferred nucleation theory of a-Ge at triple-point grain boundaries of polycrystalline Al at the interface. This discovery may be explained by the metal-induced nucleation (MIN) mechanism.

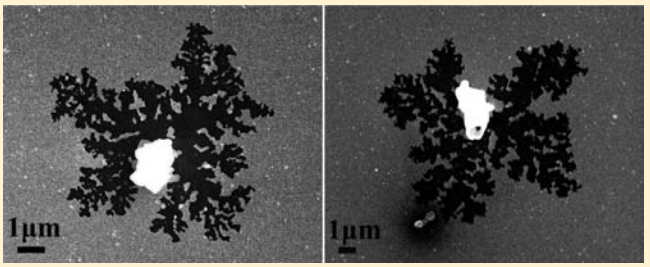

1. INTRODUCTION

Metal-induced crystallization (MIC) is a well-known phenomenon in which amorphous (a-) semiconductor films can form polycrystalline films at temperatures much lower than those required in the absence of certain metallic species.[1−5] This phenomenon has been known for several decades and is still a challenging problem from both the scientific and the technological points of view. MIC represents an alternative crystallization method for the fabrication of microelectronic devices such as thin-film transistors and solar cells.[6,7] There have been considerable reports using the MIC techniques on thin films such as a-Si, a-Ge, and a-SiGe. In most of these cases, the research has been based on layered structures in which interfacial reactions take place at amorphous semiconductor/metal films.[8−13] In the group IV semiconductors, silicon (Si) and germanium (Ge) are unique materials with a wide range of technological applications owing to their valuable semiconducting, mechanical, electrical, and optical properties in the fields of mesoscopic materials and micro-/nanodevices.[14−16] During the past several decades, there was considerable interest in the study of these semiconductors used as optical and electrical device materials.[17,18] A versatile integrated device for the semiconductor industry is highly desirable for advanced applications. Despite the fact that the use of Ge is not as extensive as that of Si, nebulous domains in our understanding of its precise technical functions still remain. Compared with the conventional Si materials, Ge has several unique properties, such as larger dielectric constant and smaller carrier mass.[19] In addition, it is known that Ge has an excitonic Bohr radius of 24.3 nm, which is much larger than that of silicon (4.9 nm).[20] Due to higher carrier mobility[21] and a lower crystallization temperature[12] than polycrystalline-Si (p-Si), p-Ge may be a potential material that can replace p-Si in thin film transistors and three-dimensional integrated circuits.[22] Therefore, it is necessary to broaden the study on the behavior of a-Ge crystallization.

Metal/Ge bilayer films with interesting micro-/nanostructured fractal Ge clusters are a nonequilibrium disordered growth system, which are accompanied by crystallization of a-Ge and formation of fractal structure.[4,23] These fractal Ge clusters exhibit charming noninteger dimensional micro-/nanostructures, which differ from those of conventional integer dimensional materials such as one-dimensional nanowires/nanorods, nanotubes, nanobelts/nanoribbons, two-dimensional heterojunctions, thin films, and zero-dimensional nanoparticles.

Received: May 20, 2012
Published: July 17, 2012

   dx.doi.org/10.1021/ic301046z | *Inorg. Chem.* 2012, 51, 8473−8478

It is expected that these films with the charming fractal Ge clusters may constitute important building blocks for micro-/nanodevices and offer exciting opportunities for both fundamental research and technological applications. Extensive literature investigations indicate that the annealing temperature plays an important role in metal/semiconductor thin films. With increasing annealing temperature and time, tensile stress often increases in the Ge layer.[24] This stress can usually be released by a reduction in the grain boundary energy of crystalline-Ge (c-Ge) due to continuous grain growth. Interestingly, the crystallization processes of a-Ge are usually accompanied by the formation of fractal Ge clusters with charming micro-/nanostructures when the films were annealed at various temperatures and times via metal-induced nucleation (MIN) mechanism.[25]

In this paper, we will describe in detail the results of an investigation on the crystallization processes of Al-induced a-Ge using a variety of analytical techniques. The fractal Ge clusters in Al/Ge bilayer films could be successfully fabricated by thermal annealing in N_2 atmosphere. Experimental results indicate that, after the films were annealed at 400 and 500 °C for 60 min, a big Al grain was found located near the center of a fractal Ge cluster. This suggests that the grain boundaries of polycrystalline Al films are the initial nucleation sites of a-Ge. It also validates the preferred nucleation theory of a-Ge at triple-point grain boundaries of polycrystalline Al at the interface. This interesting discovery may be explained by the MIN mechanism.

2. EXPERIMENTAL SECTION

Specimens were prepared on a freshly cleaved single-crystal silicon (100) substrate by evaporation in vacuum chamber at a pressure of 2.67×10^{-3} Pa at room temperature. We deposited germanium (Ge) at first and then aluminum (Al) by evaporating high-purity Ge (99.9999%) and Al (99.9%) from two resistive-heated molybdenum boats. The evaporation rate was controlled by adjusting the magnitudes of voltage and current. The deposition rates of Al and Ge films were 5 to 10 Å/s and 0.5 to 1 Å/s, respectively. The bottom layer was amorphous Ge (a-Ge), and the top one was polycrystalline Al (p-Al). The thicknesses of the p-Al and a-Ge films were 40 and 45 nm, respectively. The as-deposited samples were annealed at 200 °C, 250 °C, 300 °C, 400 °C, and 500 °C for 60 min in an atmosphere of nitrogen. The furnace heating program included a heat up period from room temperature to the target temperature with temperature increasing at 5 °C/min. When the annealing temperature reached the target temperature, the samples were annealed for 60 min, followed by natural cooling to room temperature under a continuous flow of nitrogen.

The microstructural characteristics of the as-deposited Al/a-Ge bilayer films and annealed films were investigated by scanning electron microscopy (SEM), energy dispersive X-ray spectrometry (EDS), X-ray diffraction (XRD), atomic force microscopy (AFM), and Raman scattering spectroscopy. The surface topographies of Al/Ge bilayer films were examined by a JSM-6700F scanning electron microscope and a SPM-9600 atomic force microscope. The composition of the observed regions is analyzed by energy dispersive X-ray spectrometry. XRD patterns were obtained with a Rigaku D/max-2500 diffractometer using Cu Kα radiation. The Raman measurements were carried out at room temperature, and a HeNe laser was employed in the backscattering geometry. By such annealing, self-similar fractal Ge clusters may be formed in these annealed films. Since the annealing temperatures can effectively control the morphology of the fractal patterns, the density of the different fractal clusters formed at a given annealing temperature was also approximately uniform at different sites of the sample. The average value of the evaluated dimension obtained from different regions can be approximately considered as the whole sample's fractal dimension (D). The fractal dimension for these samples was calculated by measuring the fractal dimensions of these self-similar clusters using a conventional box-counting method.[26−28]

3. RESULTS AND DISCUSSION

The SEM surface morphologies of Al/Ge bilayer films before and after annealing at different temperatures are shown in Figure 1. As seen in the SEM image shown in Figure 1a, the as-deposited Al/a-Ge bilayer film is homogeneous in morphology. In the bilayer film, the bottom layer was the Ge sublayer (45 nm) and the top one was the Al sublayer (40 nm). We can see many tiny Al nanocrystals (white regions) on the surface of the as-deposited Al/a-Ge bilayer film. After annealing in N_2 atmosphere, the Al grains gradually agglomerated to form larger grains as shown in Figure 1b, and the crystalline Ge (c-Ge) aggregates appeared on the surface of annealed films as shown in Figure 1c−e (black regions). The annealing could directly provide the thermal activation energy for Al and Ge atoms and contributed greatly to the interdiffusion of Al and Ge atoms. After the annealing temperature had reached 400 °C, the fractal Ge cluster (black regions) with open and fine branching formed on the surface of the annealed film as shown in Figure 1d. When the annealing temperature reached 500 °C, the interconnection fractal Ge clusters with dense and coarse branching appeared on the surface of the annealed film as shown in Figure 1e. Interestingly, a big Al grain was found located near the center of a fractal Ge cluster when the films were annealed at 400 and 500 °C for 60 min as shown in Figures 1d, and 4a,d. This suggests that the grain boundaries of

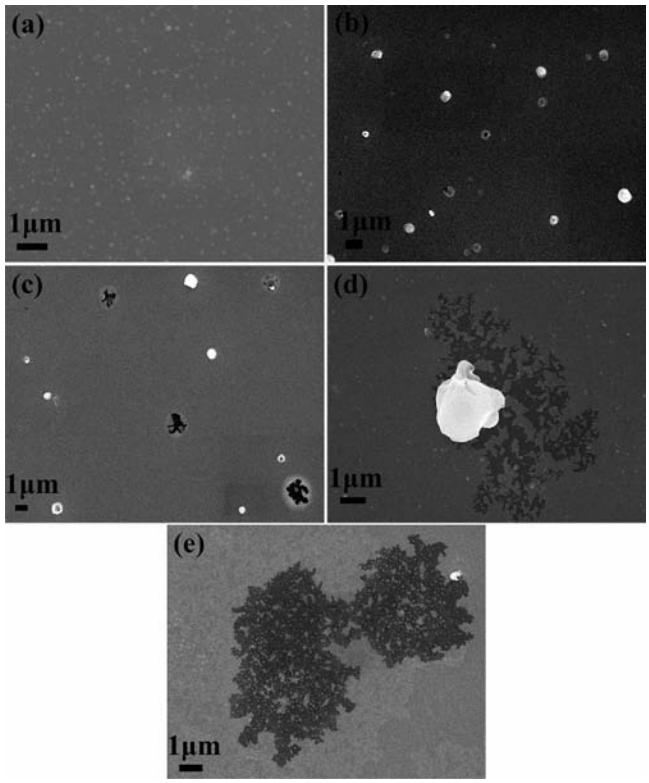

Figure 1. SEM images of the surface morphologies of Al/Ge bilayer films before and after annealing at different temperatures. (a) As-deposited, (b) annealing at 200 °C for 60 min, (c) annealing at 300 °C for 60 min, (d) annealing at 400 °C for 60 min, and (e) annealing at 500 °C for 60 min.

dx.doi.org/10.1021/ic301046z | Inorg. Chem. 2012, 51, 8473−8478

polycrystalline Al films may be the initial nucleation sites of a-Ge. The SEM images indicate that annealing at 200 and 300 °C (Figure 1b,c) did not cause significant structural change in the samples except for a slight Al grain growth and the appearance of tiny irregular Ge patterns. When the annealing temperatures reached 400 and 500 °C (Figure 1d,e), fractal Ge clusters with branching manifested on the surface of the annealed films. The experimental results indicate that interdiffusion between the Al and the Ge atoms in the matrix occurred after annealing. Surprisingly, we found that the Al and Ge sublayers had extensively exchanged their positions in the annealed films since the Al sublayer was at the top of the Ge sublayer in the as-deposited Al/a-Ge bilayer films before annealing. This phenomenon was also reported in amorphous Si/Al bilayer films by Mittemeijer et al.[29,30]

Figure 2 shows X-ray diffraction (XRD) patterns of Al/a-Ge bilayer films prepared on Si (100) substrate at room

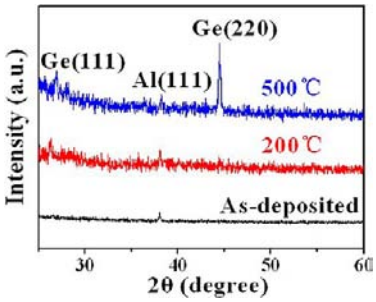

Figure 2. XRD patterns of the Al/Ge bilayer films with the as-deposited and annealed at 200 and 500 °C for 60 min.

temperature and annealed at 200 and 500 °C for 60 min. An Al (111) peak can be observed at 2θ of ~38°. No characteristic peaks belonging to other Al lattice planes or Ge crystals or impurities were detected in the as-deposited film. This indicates the amorphous structure of the Ge sublayer in the as-deposited Al/a-Ge bilayer films. After annealing at 200 °C for 60 min, a typical Ge (111) peak at 2θ of ~27° appeared in the XRD pattern. The results indicate that the Al-induced amorphous Ge sublayer begins to partially crystallize. At the higher annealing temperature treatment of 500 °C for 60 min, a typical Ge (220) diffraction peak at 2θ of ~45° appeared in the XRD pattern. The Ge (111) peak at 2θ of ~27° can also be observed. This result indicates preferred (220) orientation nucleation and (111) growth of the a-Ge crystal when the Al/Ge bilayer film was annealed at 500 °C for 60 min. This is a new finding different from the results reported in the literature on Ge (111) orientation.[30,31] After comparison of the SEM and XRD results, we believe that the Al and Ge sublayers partly exchanged their positions at the same time to accommodate the interdiffusion of the Al and Ge atoms and the formation of fractal Ge clusters during the crystallization of Al-induced a-Ge at thermally activated processes driven by the a-Ge to c-Ge phase transformation.

Figure 3 shows a typical SEM image (Figure 3a) and the atomic force microscopy (AFM) images (Figure 3b,c) of an Al/Ge bilayer film annealed at 400 °C for 60 min. Comparison of these images revealed that the observed nanostructures show interesting micro-/nanostructured fractal features. From the AFM topographic images, the variation of fractal shape, size, and density can be clearly observed. Several fractal Ge clusters are visible in Figure 3a,b. In Figure 3c, the average diameter (L)

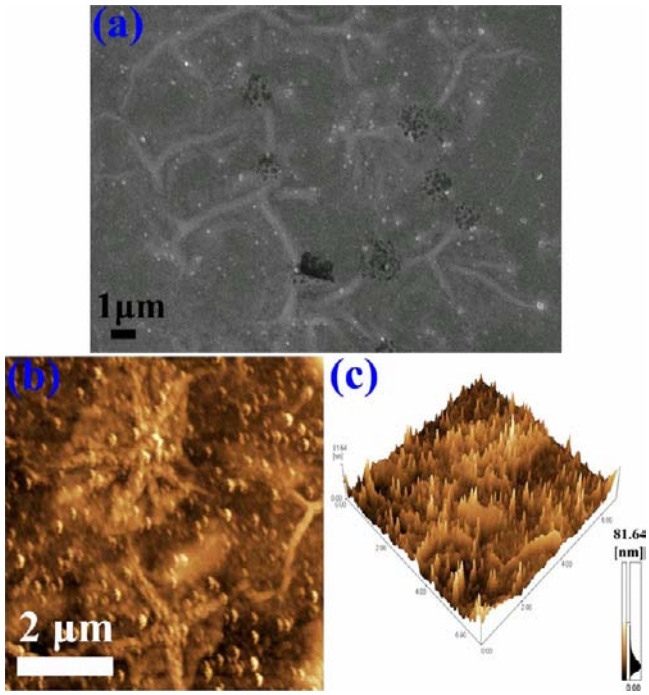

Figure 3. SEM (a) and AFM (b) images of the Al/Ge bilayer films annealed at 400 °C for 60 min and the corresponding three-dimensional AFM image (c).

and height (h) of a larger fractal Ge cluster is L = ~4 μm and h = ~81.64 nm. This fractal Ge cluster with noninteger dimensional nanostructure is referred to as nanofractal.[32] The above experimental results reveal that the annealed films show inhomogeneous distribution because of the layer exchange.

Figure 4a,d presents SEM images of Al/Ge bilayer films annealed at 400 and 500 °C for 60 min, respectively. These SEM images show that the films display interesting fractal Ge patterns at the annealing temperature due to the crystallization of a-Ge accompanied by the temperature-induced assemblies of Ge nanocrystals. To our surprise, we can clearly see a big bright Al grain on each fractal pattern, such as Figures 1d and 4a,d. Energy dispersive X-ray spectroscopy (EDS) results shown in Figure 4b,e confirmed that the big bright grain was polycrystalline Al while the black fractal branches were crystalline Ge rich regions. The Si signal originated from the Si substrate. The results also suggest that crystallization of a-Ge occurred in the surrounding of Al grains. This fact is in agreement with the theory that successive c-Ge nucleation takes place near the tip region of a fractal and that Al grain boundaries are the preferred Ge nucleation sites.[25] It is apparent that the Al grain size becomes larger when the temperature is increased. Our results imply that the metal phase plays an important role in metal-mediated crystallization (MIC). It also supports the theory that the nucleation sites of a-Ge are triple-point grain boundaries of Al at the interface of Al/Ge bilayer films. Figure 4c,d,f show the plots of $\ln(N)$ versus $\ln(1/L)$ of the fractal Ge cluster regions corresponding to Figure 4a,d, where L is the box size and N is the number of boxes occupied by the fractal Ge clusters. It can be seen that all plots show good linear relationship, which means that the morphologies of crystalline Ge clusters have scale invariance within these ranges, so these Ge patterns can be regarded as fractals. In order to obtain the fractal dimension (D), we fit a linear relationship for the function $\ln(N)$ versus $\ln(1/L)$. The results show the fractal dimension D = 1.82 in

dx.doi.org/10.1021/ic301046z | Inorg. Chem. 2012, 51, 8473−8478

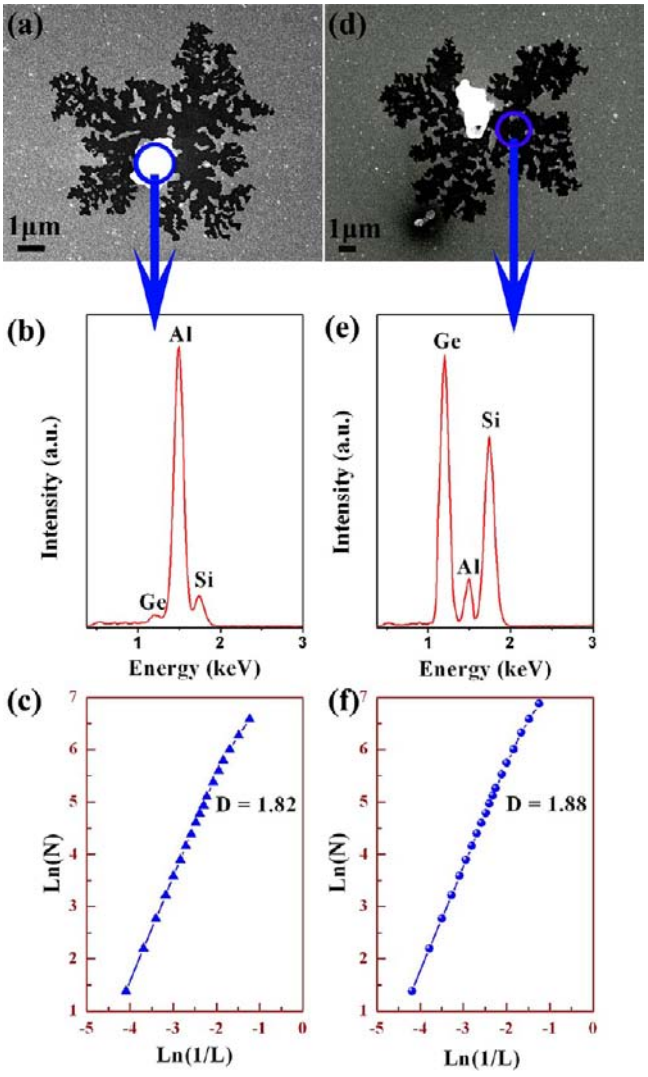

Figure 4. SEM images of the Al/Ge bilayer films annealed at (a) 400 °C and (d) 500 °C for 60 min. The corresponding EDS curves give the compositional distributions of Al and Ge as shown in parts b and e. The fractal dimensions (D) are shown parts c and f, where L is the box size and N is the number of boxes occupied by Ge cluster.

Figure 4c and 1.88 in Figure 4f. A smaller fractal dimension means that the films are composed of the open and loose fractal structure with fine branches. The open fractal patterns show thick branches and smooth edges with noninteger dimensional nanostructures, which are different from the morphology of the integer dimensional nanostructures. This is a piece of conclusive evidence that the fractal dimension of nanomaterials could be a noninteger.

Figure 5 shows the Raman scattering spectra of Al/a-Ge bilayer films in the as-deposited condition and after different annealing treatments at 200 °C, 250 °C, 300 °C, and 500 °C for 60 min. As seen in the figure, the a-Ge gradually crystallized with increasing annealing temperature. Broad spectral peaks were obtained for bilayer films annealed at a temperature below 500 °C. The characteristic peak of c-Ge appears at about 270 cm^{-1}. The Raman signals of the samples thermally treated at 200 °C, 250 °C, and 300 °C are similar. However, at an annealing temperature of 500 °C, the crystalline mode of the c-Ge peak appears at about 300 cm^{-1}, corresponding to Ge−I (diamond-cubic structure).[30] The relative intensities of the

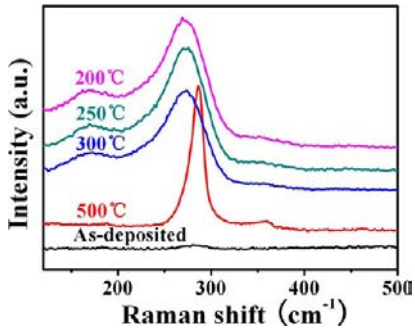

Figure 5. Raman spectra of Al/Ge bilayer films with the as-deposited and different annealing temperatures at 200 °C, 250 °C, 300 °C, and 500 °C for 60 min.

peaks at ~270 cm^{-1} and ~300 cm^{-1} correspond to the amorphous and crystalline contributions to the Raman signal. The amorphous and crystalline phases coexist in Al/Ge bilayer films with partial crystallization when the annealing temperature is below 500 °C. In conclusion, the crystallization process is gradual. The sample is almost completely crystallized after thermal treatment at 500 °C. The results from Raman spectra are in good agreement with the results obtained from SEM observations and XRD measurements.

Further advancement in the field of crystallization of a-Ge and formation of fractal Ge clusters in Al/Ge bilayer films requires a clear understanding of their formation mechanism. Metal-induced crystallization (MIC) theory has been successfully applied in previous investigations as an alternative crystallization process for thin-film device fabrication.[34,35] For example, Al,[36] Au,[37] Ag,[38] and Ni[39] have been reported to significantly decrease the crystallization temperature and time of a-Si compared to the common solid-phase crystallization (SPC) process. The silicide-forming Ni seems to be a promising candidate for thin-film transistor (TFT) fabrication by MIC.[40] Our experimental results indicate that aluminum-induced crystallization (AIC) of a-Ge can be employed to explain the formation of fractal Ge clusters: a desirable step forward in the study of metal/semiconductor bilayer films. In the present work, the Al films not only provide initial nucleation sites at triple-point grain boundaries of polycrystalline Al at Al/Ge interface but also act as important paths for Ge diffusion from amorphous regions to an already crystallized Ge region because the critical nucleation energy in the triple-point grain boundaries sites is always less than that of the flat surface. Thus, the crystallization temperature of a-Ge in Al/Ge bilayer films is lower than that of the isolated Ge films. It also validates the preferred nucleation theory of a-Ge at triple-point grain boundaries of polycrystalline Al at the interface. Although the Al/Ge interaction has been investigated extensively in the past, it remains a phenomenon apparently not well understood, especially in the case of complete Al and Ge layer exchange during AIC. The proposed formation of polycrystalline Ge films on foreign substrates by AIC relies on the overall layer exchange of adjacent Ge and Al films during the transformation of amorphous to polycrystalline Ge. The general driving force behind metal-induced crystallization is the reduction of the free energy of the Ge material during the transformation of the amorphous to the crystalline phase. When a-Ge is in contact with certain metals, electronic screening of the covalent bonding in the Ge materials occurs according to Hiraki's

dx.doi.org/10.1021/ic301046z | Inorg. Chem. 2012, 51, 8473−8478

"screening model".[41] This effect weakens the Ge bonds and, therefore, facilitates the interdiffusion of the Al and Ge atoms.

4. CONCLUSIONS

In summary, fractal Ge clusters with noninteger dimensions were successfully prepared by Al-induced crystallization of a-Ge in Al/Ge bilayer films via thermal treatment in N_2 atmosphere. Experimental results indicate that the Al grain plays an important role in the crystallization behavior of Al/Ge bilayer films after annealing and in the crystallization processes of a-Ge accompanied by fractal formation of Ge nanocrystals via temperature-induced assembly. It further confirms that preferred crystallization of a-Ge occurs in the surrounding of Al grains. This fact is in agreement with the theory that successive c-Ge nucleation takes place near the tip region of a fractal and that Al grain boundaries are the preferred successive Ge nucleation sites. In addition, the Al and Ge sublayers partly exchange their positions at the same time to accommodate the interdiffusion of the Al and Ge atoms and the formation of fractal Ge clusters during the crystallization of Al-induced a-Ge at thermally activated processes driven by the a-Ge to c-Ge phase transformation. Raman analysis indicates that the relative scattering intensities of the peaks at ~270 cm^{-1} and ~300 cm^{-1} correspond to the amorphous and crystalline contributions to the Raman signal, respectively. These findings reveal new opportunities for future study of fractal Ge clusters, which may be a promising material for important constituent building blocks for micro-/nanodevices for microelectronic applications. It is expected that these nanostructures offer exciting opportunities for both fundamental research and technological applications.

AUTHOR INFORMATION

Corresponding Author

*Tel.: +86 21 66137503. Fax: +86 21 66137787. E-mail: zwchen@shu.edu.cn (Z.C.); zjiao@shu.edu.cn (Z.J.); mhwu@staff.shu.edu.cn (M.W.).

Notes

The authors declare no competing financial interest.

ACKNOWLEDGMENTS

The work described in this article was financially supported by the Shanghai Pujiang Program (Project No. 10PJ1404100), China, Key Innovation Fund of Shanghai Municipal Education Commission (Project No. 10ZZ64), National Natural Science Foundation of China (Project Nos. 11074161, 11025526, and 41073073), Science and Technology Commission of Shanghai Municipality (Project Nos. 10JC1405400, 09530501200), and Shanghai Leading Academic Discipline Project (Project No. S30109). This work was also supported by a strategic research grant (Project No. 7002554) and a grant from the City University of Hong Kong (Project No. 7008184).

REFERENCES

(1) Oki, F.; Ogawa, Y.; Fujiki, Y. *Jpn. J. Appl. Phys.* **1969**, *8*, 1056–1056.
(2) Herd, S. R.; Chaudhari, P.; Brodsky, M. H. *J. Non-Cryst. Solids* **1972**, *7*, 309–327.
(3) Chen, Z. W.; Zhang, S. Y.; Tan, S.; Tian, M. L.; Hou, J. G.; Zhang, Y. H. *Thin Solid Films* **1998**, *322*, 194–197.
(4) Chen, Z. W.; Zhang, S. Y.; Tan, S.; Hou, J. G.; Wu, Z. Q. *Appl. Phys. A: Mater. Sci. Proc.* **2004**, *78*, 603–606.
(5) Toko, K.; Nakao, I.; Sadoh, T.; Noguchi, T.; Miyao, M. *Solid-State Electron.* **2009**, *53*, 1159–1164.
(6) Fortunato, G. *Thin Solid Films* **1997**, *296*, 82–90.
(7) Shi, Z.; Green, M. A. *Prog. Photovoltaics* **1998**, *6*, 247–257.
(8) Nast, O.; Hartmann, A. J. *J. Appl. Phys.* **2000**, *88*, 716–724.
(9) Jin, Z.; Bhat, G. A.; Yeung, M.; Kwok, H. S.; Wong, M. *J. Appl. Phys.* **1998**, *84*, 194–200.
(10) Gaudet, S.; Detavernier, C.; Kellock, A.; Dejardins, P.; Lavoie, C. *J. Vac. Sci. Technol., A* **2006**, *24*, 474–485.
(11) Konno, T. J.; Sinclair, R. *Mater. Sci. Eng., A* **1994**, *179–180*, 426–432.
(12) Kanno, H.; Toko, K.; Sadoh, T.; Miyao, M. *Appl. Phys. Lett.* **2006**, *89*, 182120–182122.
(13) Knaepen, W.; Gaudet, S.; Detavernier, C.; Van Meirhaeghe, R. L.; Sweet, J. J.; Lavoie, C. *J. Appl. Phys.* **2009**, *105*, 083532–083537.
(14) Landman, U.; Barnett, R. N.; Scherbakov, A. G.; Avouris, P. *Phys. Rev. Lett.* **2000**, *85*, 1958–1961.
(15) Zhang, Y. F.; Tang, Y. H.; Wang, N.; Lee, C. S.; Bello, I.; Lee, S. T. *Phys. Rev. B* **2000**, *61*, 4518–4521.
(16) Lu, X. M.; Ziegler, K. J.; Ghezelbash, A.; Johnston, K. P.; Korgel, B. A. *Nano Lett.* **2004**, *4*, 969–974.
(17) Quartarone, E.; Mustarelli, P.; Marabelli, F.; Battagliarin, M.; Turato, S. *J. Vac. Sci. Technol., A* **2004**, *22*, 2234–2238.
(18) Szkutnik, P. D.; Sgarlata, A.; Motta, N.; Balzarotti, A. *Mater. Sci. Eng., C* **2003**, *23*, 1053–1508.
(19) Cao, Z. H.; Liu, P.; Meng, X. K.; Tang, S. C.; Lu, H. M. *Appl. Phys. A: Mater. Sci. Proc.* **2009**, *94*, 393–398.
(20) Wu, Y.; Yang, P. *Chem. Mater.* **2000**, *12*, 605–607.
(21) Schaffler, F. *Properties of silicon germanium and SiGe: Carbon*; Kasper, E., Lyutovich, K., Eds.; INSPEC: London, UK, 2000; p 198.
(22) Phung, T. H.; Zhu, C. X. *J. Electrochem. Soc.* **2010**, *157*, H755–H758.
(23) Chen, Z. W.; Zhang, S. Y.; Tan, S.; Hou, J. G.; Zhang, Y. H. *J. Vac. Sci. Technol., A* **1998**, *16*, 2292–2294.
(24) Wang, Z. M.; Wang, J. Y.; Jeurgens, L. P. H.; Phillipp, F.; Mittemeijer, E. J. *Acta Mater.* **2008**, *56*, 5047–5057.
(25) Chen, Z. W.; Lai, J. K. L.; Shek, C. H.; Chen, H. D. *Appl. Surf. Sci.* **2005**, *250*, 3–8.
(26) Chen, Z. W.; Jiao, Z.; Wu, M. H.; Shek, C. H.; Wu, C. M. L.; Lai, J. K. L. *Prog. Mater. Sci.* **2011**, *56*, 901–1029.
(27) Forrest, S. R.; Witten, T. A. *J. Phys. A: Math. Gen.* **1979**, *12*, L109–L117.
(28) Chen, Z. W.; Li, Q. B.; Pan, D. Y.; Li, Z.; Jiao, Z.; Wu, M. H.; Shek, C. H.; Wu, C. M. L.; Lai, J. K. L. *J. Phys. Chem. C* **2011**, *115*, 9871–9878.
(29) Zhao, Y. H.; Wang, J. Y.; Mittemeijer, E. J. *Appl. Phys. A: Mater. Sci. Proc.* **2004**, *79*, 681–690.
(30) Wang, Z. M.; Wang, J. Y.; Jeurgens, L. P. H.; Mittemeijer, E. J. *Phys. Rev. B* **2008**, *77*, 045424–1–15.
(31) Hu, S.; Marshall, A. F.; McIntyre, P. C. *Appl. Phys. Lett.* **2010**, *97*, 082104–082106.
(32) Chen, Z. W.; Li, Q. B.; Pan, D. Y.; Zhang, H. J.; Jiao, Z.; Wu, M. H.; Shek, C. H.; Wu, C. M. L.; Lai, J. K. L. *Mater. Today* **2011**, *14*, 106–113.
(33) Jang, J. I.; Lance, M. J.; Wen, S. Q.; Pharr, G. M. *Appl. Phys. Lett.* **2005**, *86*, 131907–131909.
(34) Nast, O.; Brehme, S.; Neuhaus, D. H.; Wenham, S. R. *IEEE Trans. Electron Devices* **1999**, *46*, 2062–2068.
(35) Nast, O.; Wenham, S. R. *J. Appl. Phys.* **2000**, *88*, 124–132.
(36) Haque, M. S.; Naseem, H. A.; Brown, W. D. *J. Appl. Phys.* **1994**, *75*, 3928–3935.
(37) Hultman, L.; Robertsson, A.; Hentzell, H. T. G.; Engström, I.; Psaras, P. A. *J. Appl. Phys.* **1987**, *62*, 3647–3655.
(38) Bian, B.; Yie, J.; Li, B. Q.; Wu, Z. Q. *J. Appl. Phys.* **1993**, *73*, 7402–7406.
(39) Jin, Z. H.; Bhat, G. A.; Yeung, M.; Kwok, H. S.; Wong, M. *J. Appl. Phys.* **1998**, *84*, 194–200.
(40) Jiang, J.; Oh, J. Y.; Kim, S. K.; Choi, Y. J.; Yoon, S. Y.; Kim, C. O. *Nature* **1998**, *395*, 481–483.

(41) Hiraki, A. *J. Electrochem. Soc.* **1980**, *127*, 2662−2665.